



COPY RIGHT

2017 IJIEMR. Personal use of this material is permitted. Permission from IJIEMR must be obtained for all other uses, in any current or future media, including reprinting/republishing this material for advertising or promotional purposes, creating new collective works, for resale or redistribution to servers or lists, or reuse of any copyrighted component of this work in other works. No Reprint should be done to this paper, all copy right is authenticated to Paper Authors

IJIEMR Transactions, online available on 23rd July 2017. Link :

<http://www.ijiemr.org/downloads.php?vol=Volume-6&issue=ISSUE-5>

Title: Performance Analysis of Novel Three Phase Power Converter Fed Induction Motor Drive Using Pv Based Parallel Rectifier Topology.

Volume 06, Issue 05, Page No: 2038 – 2041.

Paper Authors

***CHEEKATI BHAVYA, DR. N. SAMBASIVA RAO.**

* dept of EEE, NRI Institute of Technology.



USE THIS BARCODE TO ACCESS YOUR ONLINE PAPER

To Secure Your Paper As Per **UGC Guidelines** We Are Providing A Electronic Bar Code



PERFORMANCE ANALYSIS OF NOVEL THREE PHASE POWER CONVERTER FED INDUCTION MOTOR DRIVE USING PV BASED PARALLEL RECTIFIER TOPOLOGY

***CHEEKATI BHAVYA,**DR. N. SAMBASIVA RAO**

*PG Scholar, dept of EEE, NRI Institute of Technology, Andhra pradesh, India.

**Professor, dept of EEE , NRI Institute of Technology, Andhra pradesh, India.

bhavyacheekati@gmail.com

nsraohodeee@gmail.com

ABSTRACT:

In this project three phase power converter fed induction motor with PV rectifier is proposed. Solar energy is the most low cost, competition free, universal source of energy as sun shines throughout. This energy can be converted into useful electrical energy using photovoltaic technology. A single-phase to three-phase drive system composed of two parallel single-phase rectifiers, a three-phase inverter, and an induction motor. Parallel converters can be used to improve the power capability, reliability, efficiency and redundancy. Parallel converter techniques can be employed to improve the performance of active power filters, uninterruptable power supplies, fault tolerance of doubly fed induction generators and three phase drives. The proposed topology improves the better performance of the power converter. Induction motor has been operated as a work horse in the industry due to its easy build, high robustness and generally satisfactory efficiency. The Induction Motors are the AC motors and hence from converter, an inverter system is also required to obtain an AC voltage. This inverter is chosen based on its advantages and it is fed to induction motor. In this pulse width modulation technique (PWM) will be developed. The overall system performance is observed by using MATLAB/SIMULINK software.

Key words-Ac-dc-ac power converter, Induction Motor drive system, parallel Converter, Fault Identification System (FIS)

I. INTRODUCTION

Several solutions have been proposed when the objective is to supply a three-phase motor from single-phase ac mains [1]. It is quite common to have only a single phase power grid in residential, commercial, manufacturing, and mainly in rural areas, while the adjustable speed drives may request a three-phase power grid. Single-phase to three-phase ac–dc–ac conversion usually employs a full-bridge topology, which implies in ten power switches. This converter is denoted here as conventional topology. Parallel converters have

been used to improve the power capability, reliability, efficiency, and redundancy. Parallel converter techniques can be employed to improve the performance of active power filters [2-3], uninterruptible power supplies (UPS) [4], fault tolerance of doubly fed induction generators, and three-phase drives. Usually the operation of converters in parallel requires a transformer for isolation.

In this paper, a single-phase to three-phase drive system composed of two parallel single-phase rectifiers and a three phase

inverter is proposed [5-6]. The proposed system is conceived to operate where the single-phase utility grid is the unique option available. Compared to the conventional topology, the proposed system permits to reduce the rectifier switch currents, the total harmonic distortion (THD) of the grid current with same switching frequency or the switching frequency with same THD of the grid current, and to increase the fault tolerance characteristics. In addition, the losses of the proposed system may be lower than that of the conventional counterpart. The aforementioned benefits justify the initial investment of the proposed system, due to the increase of number of switches [7-8].

The 1phto-3ph converter based on a controlled rectifier is composed of five legs (ten controlled power devices), as shown in Fig. 1(a). It is denominated conventional 5L converter. In order to reduce the cost and power losses in the power converter, different configurations of 1ph-to-3ph converter with a reduced number of power devices have been proposed in the literature [9-11]. Within that range of possibility, we can highlight the configurations with four legs (composed of a full-bridge rectifier and a three-leg inverter with a shared leg) [12-13], denominated here conventional 4L converter [see Fig. 1(b)]

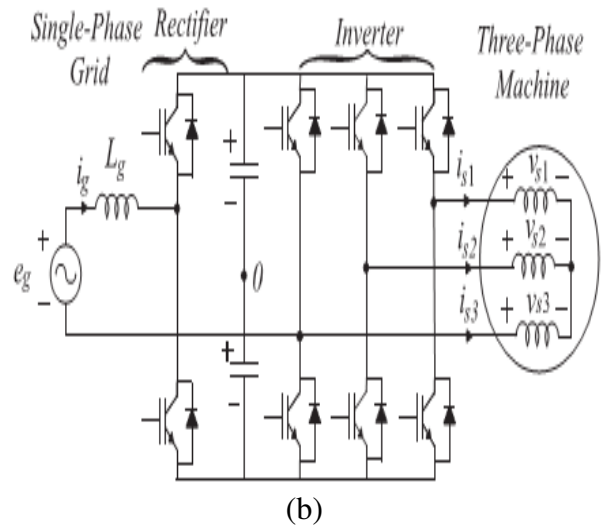
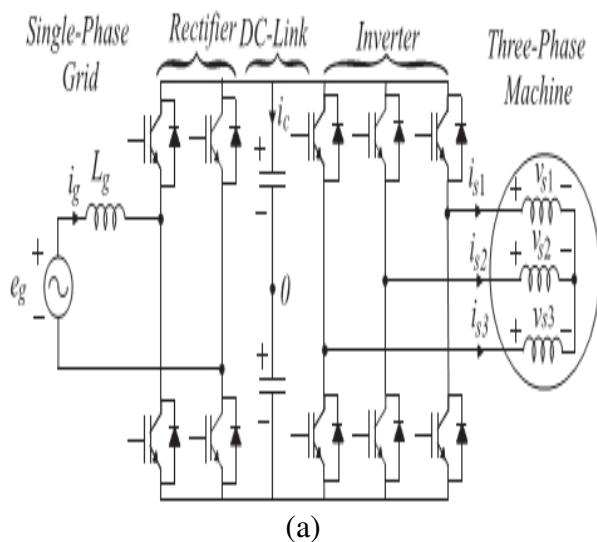


Fig.1. Conventional 1ph-to-3ph converter system (a) Five-leg (5L) converter, (b) Four-leg (4L) converter

Parallel converters have been used to improve the power capability, reliability, efficiency, and redundancy. Parallel converter techniques can be employed to improve the performance of active power filters, uninterruptible power supplies (UPS), fault tolerance of doubly fed induction generators, and three-phase drives. Usually the operation of converters in parallel requires a transformer for isolation. However, weight, size, and cost associated with the transformer may make such a solution undesirable. When an isolation transformer is not used, the reduction of circulating currents among different converter stages is an important objective in the system design.

II. SYSTEM MODEL

The P5L configuration presented in Fig.2 (a) is composed of two single-phase half-bridge rectifiers (rectifiers A and B), a dc-link, a three-phase inverter and a three-phase motor or a three-phase load. On the other hand, the P4L configuration [see Fig.2 (b)] is composed of a two-leg inverter instead three-leg inverter of the P5L converter.



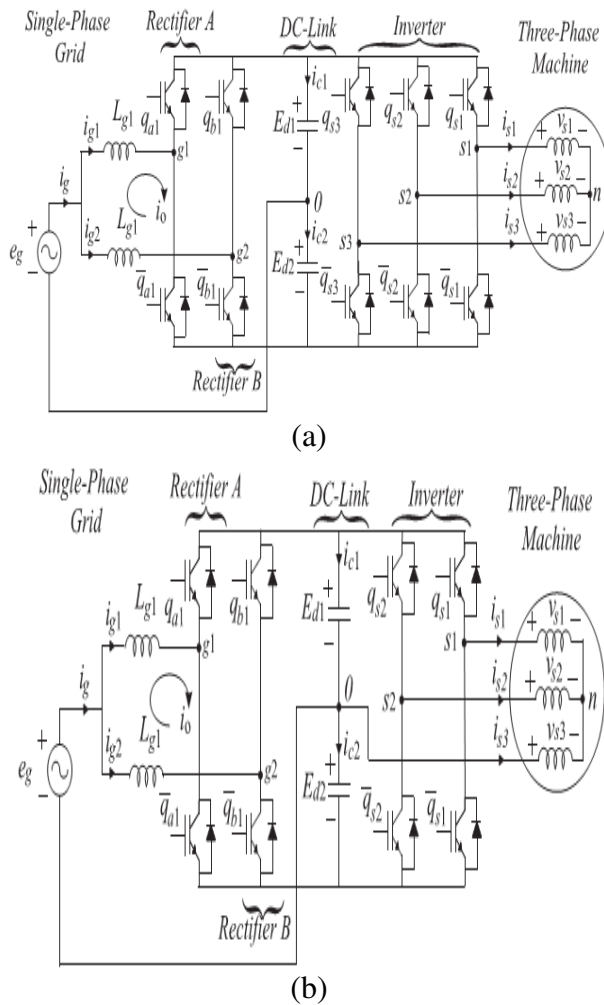


Fig.2. Proposed 1ph-to-3ph converter using a half-bridge rectifier circuit (a) Parallel five-leg (P5L) converter, (b) Parallel four-leg (P4L) converter

A) Rectifier Model

From Fig.2, the following model is derived:

$$e_g = r_{g1}i_{g1} + l_{g1} \frac{di_{g1}}{dt} + v_{g10} \quad (1)$$

$$e_g = r_{g1}i_{g2} + l_{g1} \frac{di_{g2}}{dt} + v_{g20} \quad (2)$$

$$i_g = i_{g1} + i_{g2} \quad (3)$$

Where r_{g1} represents the resistance of the inductor filter L_{g1} , l_{g1} represents the inductance of the inductor filter L_{g1} , v_{g10} , and v_{g20} are the pole voltages of the rectifiers A and B, respectively, i_g is the grid current and i_{g1} and i_{g2} are the input currents of the rectifiers A and B, respectively.

The previous model can also be expressed by using the circulating current i_o introduced by

$$i_{g1} = \frac{i_g}{2} + i_o \quad (4)$$

$$i_{g2} = \frac{i_g}{2} - i_o \quad (5)$$

From (1) to (5), the complete system model is given by

$$e_g = \left(\frac{r_{g1}}{2}\right) i_g + \left(\frac{l_{g1}}{2}\right) \frac{di_g}{dt} + v_g \quad (6)$$

$$v_o = r_{g1}i_o + l_{g1} \frac{di_o}{dt} \quad (7)$$

With

$$i_o = \frac{i_{g1} - i_{g2}}{2} \quad (8)$$

$$v_g = \frac{v_{g10} + v_{g20}}{2} \quad (9)$$

$$v_o = \frac{-v_{g10} + v_{g20}}{2} \quad (10)$$

From (6) to (10), it is clear that the grid and circulating currents depend on the voltages v_g and v_o , respectively. Then, the rectifier pole voltages can be calculated from desired voltages (v_g and v_o) to control these currents. Considering circulating current null and the equivalent inductor $L_g = L_{g1}/2$ equal to that of the conventional converter, the front-end model of the configurations presented in Fig.2 is identical to that of the conventional 5L converter.

B) Inverter Model

The inverter model for the P5L configuration is given by

$$v_{s1} = v_{s10} - v_{n0} \quad (11)$$

$$v_{s2} = v_{s20} - v_{n0} \quad (12)$$

$$v_{s3} = v_{s30} - v_{n0} \quad (13)$$

Where v_{s10} , v_{s20} , and v_{s30} are the pole voltages of the inverter, v_{s1} , v_{s2} , and v_{s3} are the voltages of the three-phase load, and v_{n0} is the voltage between the point n and the dc-link midpoint 0 . While the model of inverter of the P4L configuration is given by

$$v_{s13} = v_{s10} \quad (14)$$

$$v_{s23} = v_{s20} \quad (15)$$

Where v_{s13} and v_{s23} are line voltages of the three-phase load.

III. CONTROL STRATEGY

The control system of the proposed converters has the same objectives of the conventional one, i.e., dc-link voltage and power factor control from rectifier circuit and load voltage control from inverter circuit. Additionally, the proposed control system needs to regulate the circulating current between the parallel half-bridge rectifiers. Fig.3 shows the control block diagram of the P5L and P4L converters proposed in this paper. The capacitor dc-link voltage E_d ($E_{d1} + E_{d2}$) is adjusted to its reference value E_d^* utilizing a proportional integral (PI) type controller. This controller provides the amplitude of the reference grid current I_g^* . To control power factor and harmonics at the grid side, the instantaneous reference grid current i_{gx}^* must be synchronized with the grid voltage e_g based on phase locked loop scheme. Control of the grid current is implemented using a synchronous controller (a resonant controller type) described. The block R_g represents this controller. It defines the reference grid voltage v_g^* .

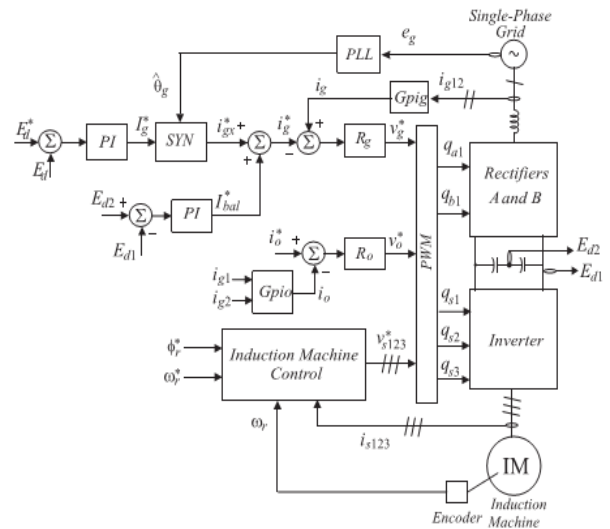


Fig.3. Control block diagram used for configurations P5L and P4L.

The circulating current (i_o) is obtained by block G_{pio} from the measured rectifiers currents i_{g1} and i_{g2} . This block is based on (8). The circulating current is compared to its reference ($i_o^* = 0$). The error is the input of a synchronous controller (R_o), and gives in its output the voltage v_o^* . Due to different dead-time switches, nonsinusoidal grid voltage or different capacitance, the voltage balance between the split capacitors obtained naturally may not be satisfactory. Some works have proposed solutions to voltage balance between the split capacitors of the half-bridge rectifier. One way to minimize the voltage imbalance between split capacitors is to add a current balance value i_{bal}^* in the reference grid current. The difference in voltage between the split capacitors ($E_{d1} - E_{d2}$) is input of the conventional PI controller. This controller provides the reference current balance value (i_{bal}^*). The reference grid current is achieved by adding i_{gx}^* with i_{bal}^* ($i_g^* = i_{gx}^* + i_{bal}^*$), as discussed. The voltage balance between the split capacitors is carried out, but it is necessary to apply a small distortion in the reference grid current. When a three-phase motor is used, control can be performed by the field-oriented

control (FOC) technique as shown or volt/hertz control.

IV. PWM STRATEGY

The PWM methods can be based on classic sinusoidal modulation, scalar as well as on vector modulation approach. In sinusoidal modulation, the gating signals are obtained by comparing reference pole voltages with a triangular carrier signal. In this paper, the PWM strategy for the rectifiers A and B will be based on sinusoidal modulation. The gating signals are obtained by comparing reference pole voltages with one or two high-frequency triangular carrier signals, i.e., a single or double carriers PWM implementation. In the case of double carrier approach (interleaved technique), the phase shift of the two triangular carrier signals is 180° . The reference pole voltages of the rectifiers are obtained as follows.

Considering that v_g^* and v_o^* are the reference voltages determined by the current controllers, from (9) and (10), we found

$$v_g^* = \frac{v_{g10}^* + v_{g20}^*}{2} \quad (16)$$

$$v_o^* = \frac{-v_{g10}^* + v_{g20}^*}{2} \quad (17)$$

Writing (16) and (17) in matrix form

$$\begin{bmatrix} v_g^* \\ v_o^* \end{bmatrix} = \frac{1}{2} \begin{bmatrix} 1 & 1 \\ -1 & 1 \end{bmatrix} \begin{bmatrix} v_{g10}^* \\ v_{g20}^* \end{bmatrix} \quad (18)$$

The gating signals are directly calculated from the reference pole voltages (v_{g10}^* and v_{g20}^*), solving (18), we obtain

$$v_{g10}^* = v_g^* - v_o^* \quad (19)$$

$$v_{g20}^* = v_g^* + v_o^* \quad (20)$$

Suitable modulation is obtained when $-E_d^*/2 \leq v_{g10}^* \leq E_d^*/2$ and $-E_d^*/2 \leq v_{g20}^* \leq E_d^*/2$. Where

E_d^* is the reference dc-link voltage with $E_d^* = E_{d1}^* + E_{d2}^*$. The three-phase inverter (P5L configuration) can be commanded by using an adequate PWM strategy for the three-phase voltage source inverter. While for the two-leg inverter (P4L converter), the PWM can be obtained with a similar technique presented.

V. DC-LINK CAPACITOR

A) DC-Link Capacitor Voltage

Considering that all the voltages are purely sinusoidal, the voltage limits conditions of each configuration. Where V_g represents the amplitude of rectifier voltage, whereas V_s denotes the amplitude of the load phase voltage. If the input voltage is equal to output voltage (i.e., $V_g = V_s$), the conventional 5L converter has the best dc-link voltage rating. The proposed P5L converter has the dc-link voltage 15% bigger than the conventional 5L one. While conventional 3L and proposed P4L converters require twice the dc-link voltage of the conventional 5L one.

On the other hand, when the output voltage is double the input voltage (i.e., $V_s = 2V_g$), the proposed P5L converter can operate with the same dc-link voltage of the conventional 5L converter.

B) DC-Link Capacitor Current

From Fig.2 (a), the dc-link capacitor current for the P5L converter can be given by

$$i_{c1} = \sum_{k=1}^2 \frac{\tau_{gk}}{T_s} i_{gk} - \sum_{j=1}^3 \frac{\tau_{sj}}{T_s} i_{sj} \quad (21)$$

$$i_{c2} = -\sum_{k=1}^2 \left(1 - \frac{\tau_{gk}}{T_s}\right) i_{gk} + \sum_{j=1}^3 \left(1 - \frac{\tau_{sj}}{T_s}\right) i_{sj} \quad (22)$$

Where τ_{gk} and τ_{sj} are the time intervals in which switches q_{gk} and q_{sj} are closed (with $k = 1, 2$ and $j = 1, 2, 3$), respectively, and T_s is the sampling time. Assuming that the reference pole voltages are constant over T_s , the time intervals τ_{gk} and τ_{sj} can be written as a function of the reference pole voltages. For instance, τ_{gk} is given by

$$\tau_{gk} = \left(\frac{v_{gk0}^*}{E_d^*} + \frac{1}{2} \right) T_s \quad (23)$$

Thus, from (21)–(23), the dc-link capacitor current is given by

$$i_{c1} = \frac{i_g}{2} + \sum_{k=1}^2 \frac{v_{gk0}^*}{E_d^*} i_{gk} - \sum_{j=1}^3 \frac{v_{sj0}^*}{E_d^*} i_{sj} \quad (24)$$

$$i_{c2} = -\frac{i_g}{2} + \sum_{k=1}^2 \frac{v_{gk0}^*}{E_d^*} i_{gk} - \sum_{j=1}^3 \frac{v_{sj0}^*}{E_d^*} i_{sj} \quad (25)$$

If the reference pole voltages are defined by (19) and (20) and the rectifier currents by (4) and (5), then the capacitor currents i_{c1} and i_{c2} can be written as follows:

$$i_{c1} = \frac{i_g}{2} + \frac{v_g^*}{E_d^*} i_g - \frac{2v_o^*}{E_d^*} i_o - \sum_{j=1}^3 \frac{v_{sj}^*}{E_d^*} i_{sj} \quad (26)$$

$$i_{c2} = -\frac{i_g}{2} + \frac{v_g^*}{E_d^*} i_g - \frac{2v_o^*}{E_d^*} i_o - \sum_{j=1}^3 \frac{v_{sj}^*}{E_d^*} i_{sj} \quad (27)$$

The first component of the capacitor currents, for the P5L converter, is due to the grid connection at the midpoint of the dc-link, the second component is due to the single-phase voltage source, with twice of the grid frequency. The third component is a consequence of the circulating current. Although there is no low-frequency circulating current (eliminated by the controller), it may exist with high-frequency circulating current due to the interleaving technique. The last term is due to the three-phase inverter. A similar analysis may be obtained with the P4L converter, but in this case, there is a load current component (i_{s3}) due to the load connection at the midpoint dc-link, as shown in the following equations:

$$i_{c1} = \frac{i_g}{2} + \frac{i_{s3}}{2} + \frac{v_g^*}{E_d^*} i_g - \frac{2v_o^*}{E_d^*} i_o - \sum_{j=1}^2 \frac{v_{sj0}^*}{E_d^*} i_{sj} \quad (28)$$

$$i_{c2} = -\frac{i_g}{2} - \frac{i_{s3}}{2} + \frac{v_g^*}{E_d^*} i_g - \frac{2v_o^*}{E_d^*} i_o - \sum_{j=1}^2 \frac{v_{sj0}^*}{E_d^*} i_{sj} \quad (29)$$

Another common feature among the studied configurations is a component in frequency of 120 Hz due to a single-phase power supply. Moreover, the proposed configurations have a reduction at high-frequency components in capacitor currents, especially when double-carrier PWM is applied. For instance, the RMS capacitor current of the P5L converter (with interleaved technique) decreases by 33% compared to the conventional 5L converter.

VI. HARMONIC DISTORTION

In this paper, the weighted total harmonic distortion factor (WTHD) has been used to evaluate the distortion of the converter voltage, because it is superior to the total harmonic distortion factor to measure the quality of a non sinusoidal waveform. The WTHD is defined by

$$WTHD = \frac{\sqrt{\sum_{h=2}^{N_h} \left(\frac{V_h}{V_1} \right)^2}}{V_1} \quad (30)$$

Where V_1 is the amplitude of the fundamental voltage component, V_h is the amplitude of h th component voltage harmonic, and N_h is the number of harmonics taken into consideration.

VII. CONVERTER LOSSES

Several studies have been performed in order to determine the power losses in the power switches (IGBTs and MOSFETs). Two solutions are generally applied: 1) the experimental measurement of power loss, with the aim of constructing mathematical functions from a regression model and 2) determining losses using linear IGBT and diode models. In this paper, the losses estimation is obtained through of the regression model, which has been achieved by experimental tests. The tests were performed for different values of currents and temperatures. All data of losses have been employed to obtain the regression model, as

presented. Such a regression model provides polynomial equations for the losses.

The instantaneous losses function of an IGBT dual module CM50DY-24H manufactured by POWEREX driven by driver SKHI-10 manufactured by SEMIKRON was determined. Then, digital simulation provided by PSIM simulation software was used to calculate the power losses in converters. The polynomial equations were implemented using a DLL (dynamic-link library) written in C (programming language).

VIII. INDUCTION MOTOR

An asynchronous motor type of an induction motor is an AC electric motor in which the electric current in the rotor needed to produce torque is obtained by electromagnetic induction from the magnetic field of the stator winding. An induction motor can therefore be made without electrical connections to the rotor as are found in universal, DC and synchronous motors. An asynchronous motor's rotor can be either wound type or squirrel-cage type.

Three-phase squirrel-cage asynchronous motors are widely used in industrial drives because they are rugged, reliable and economical. Single-phase induction motors are used extensively for smaller loads, such as household appliances like fans. Although traditionally used in fixed-speed service, induction motors are increasingly being used with variable-frequency drives (VFDs) in variable-speed service. VFDs offer especially important energy savings opportunities for existing and prospective induction motors in variable-torque centrifugal fan, pump and compressor load applications. Squirrel cage induction motors are very widely used in both fixed-speed and variable-frequency drive (VFD) applications. Variable voltage and variable frequency drives are also used in variable-speed service.

In both induction and synchronous motors, the AC power supplied to the motor's

stator creates a magnetic field that rotates in time with the AC oscillations. Whereas a synchronous motor's rotor turns at the same rate as the stator field, an induction motor's rotor rotates at a slower speed than the stator field. The induction motor stator's magnetic field is therefore changing or rotating relative to the rotor. This induces an opposing current in the induction motor's rotor, in effect the motor's secondary winding, when the latter is short-circuited or closed through external impedance. The rotating magnetic flux induces currents in the windings of the rotor; in a manner similar to currents induced in a transformer's secondary winding(s). The currents in the rotor windings in turn create magnetic fields in the rotor that react against the stator field. Due to Lenz's Law, the direction of the magnetic field created will be such as to oppose the change in current through the rotor windings. The cause of induced current in the rotor windings is the rotating stator magnetic field, so to oppose the change in rotor-winding currents the rotor will start to rotate in the direction of the rotating stator magnetic field. The difference, or "slip," between actual and synchronous speed varies from about 0.5 to 5.0% for standard Design B torque curve induction motors. The induction machine's essential character is that it is created solely by induction instead of being separately excited as in synchronous or DC machines or being self-magnetized as in permanent magnet motors.

For rotor currents to be induced the speed of the physical rotor must be lower than that of the stator's rotating magnetic field (n_s); otherwise the magnetic field would not be moving relative to the rotor conductors and no currents would be induced. As the speed of the rotor drops below synchronous speed, the rotation rate of the magnetic field in the rotor increases, inducing more current in the windings and creating more torque. The ratio between the rotation rate of the magnetic field

induced in the rotor and the rotation rate of the stator's rotating field is called slip. Under load, the speed drops and the slip increases enough to create sufficient torque to turn the load.

Synchronous Speed:

The rotational speed of the rotating magnetic field is called as synchronous speed.

$$N_s = \frac{120 \times f}{P} \quad (\text{RPM}) \quad (31)$$

Where,

f = frequency of the supply

P = number of poles

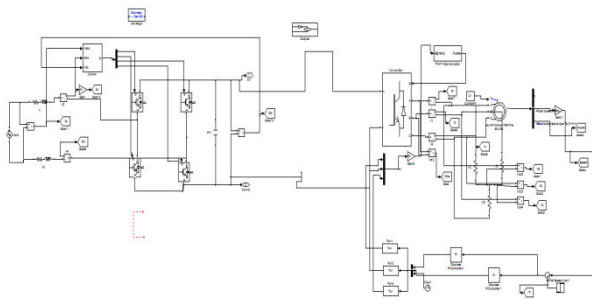
Slip:

Rotor tries to catch up the synchronous speed of the stator field, and hence it rotates. But in practice, rotor never succeeds in catching up. If rotor catches up the stator speed, there won't be any relative speed between the stator flux and the rotor, hence no induced rotor current and no torque production to maintain the rotation. However, this won't stop the motor, the rotor will slow down due to lost of torque, and the torque will again be exerted due to relative speed. That is why the rotor rotates at speed which is always less the synchronous speed.

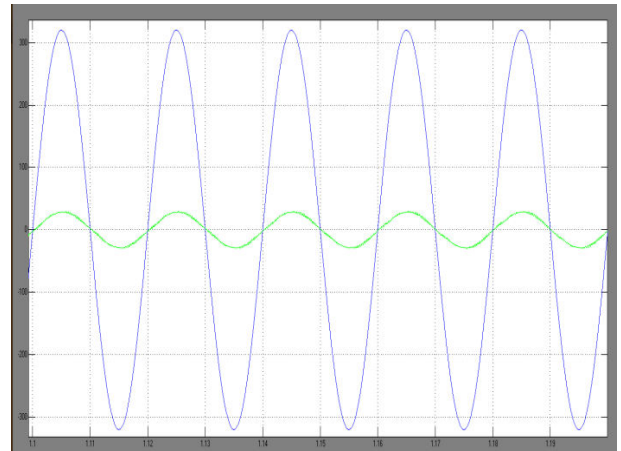
The difference between the synchronous speed (N_s) and actual speed (N) of the rotor is called as slip.

$$\% \text{ slip } s = \frac{N_s - N}{N_s} \times 100 \quad (32)$$

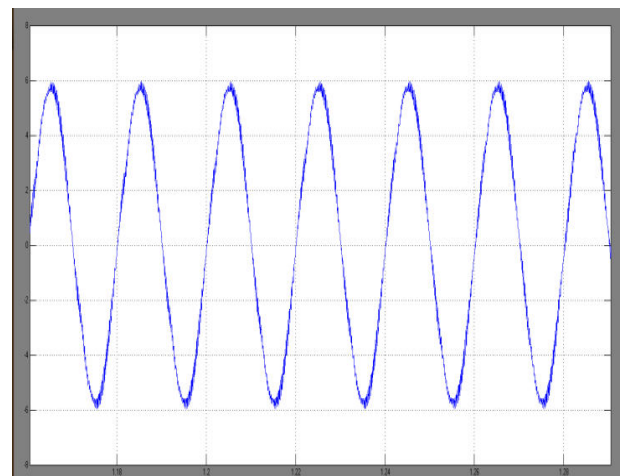
IX. MATLAB/SIMULINK RESULTS



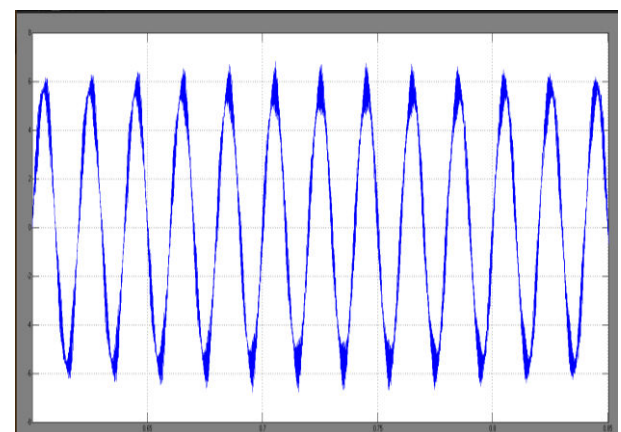
MATLAB/SIMULINK circuit for 1ph-to-3ph converter using a half-bridge rectifier with Parallel five-leg converter



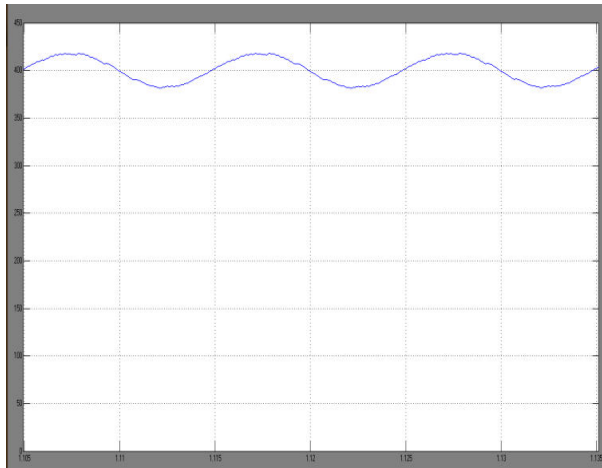
Voltage and current output waveform



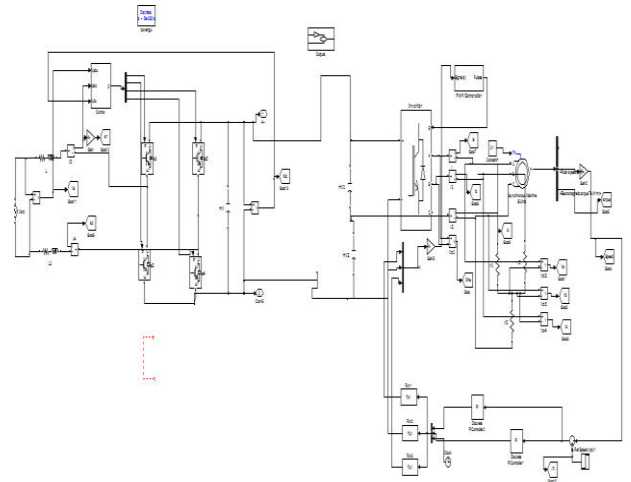
Rectifier Input Current i_{g1}



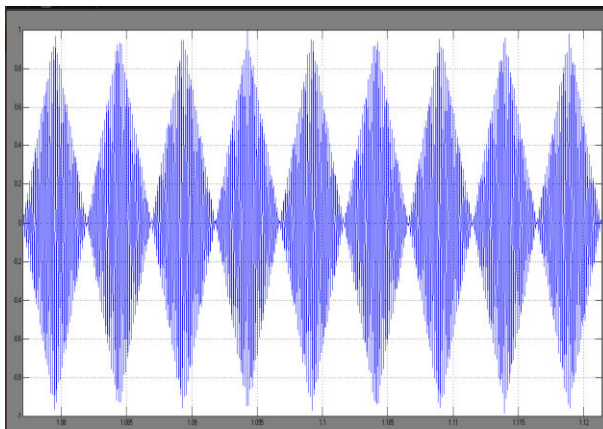
Rectifier Input Current i_{g2}



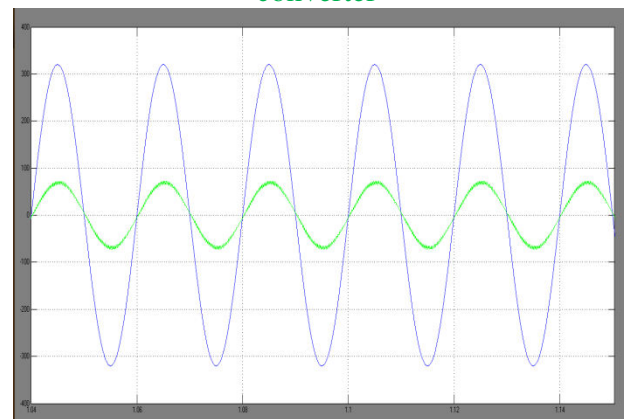
Dc-link total output voltage



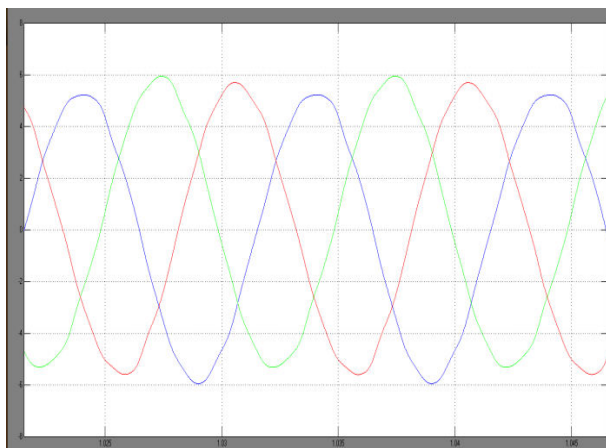
MATLAB/SIMULINK circuit for 1ph-to-3ph converter using a half-bridge rectifier with Parallel four-leg converter



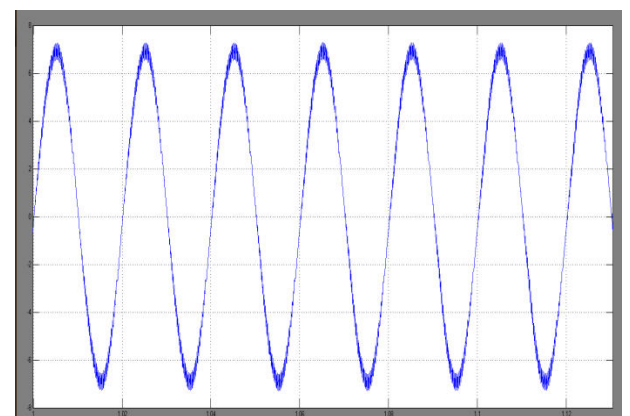
Circulating current



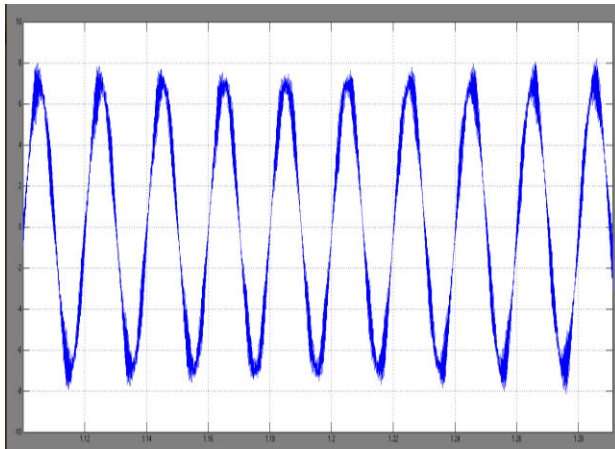
Voltage and Current



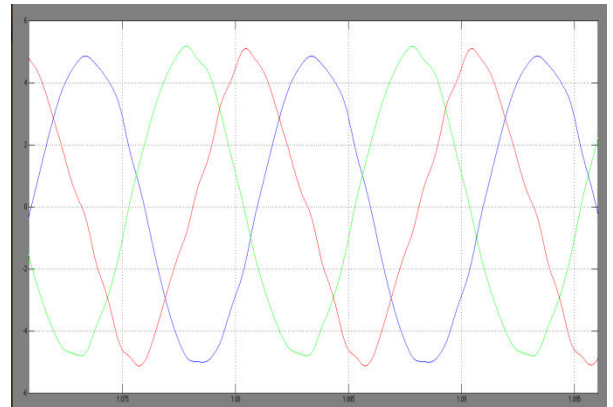
Load currents i_{s1} , i_{s2} and i_{s3}



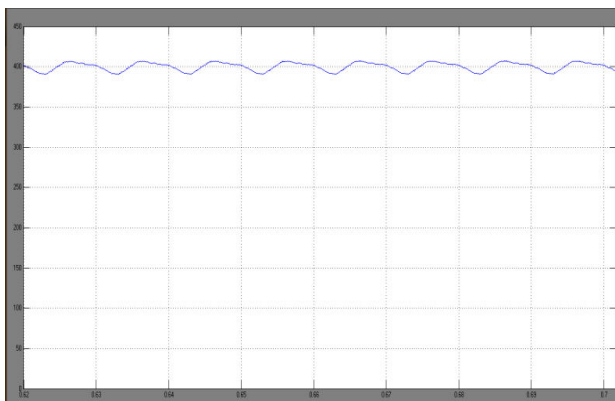
Rectifier Input Current i_{g1}



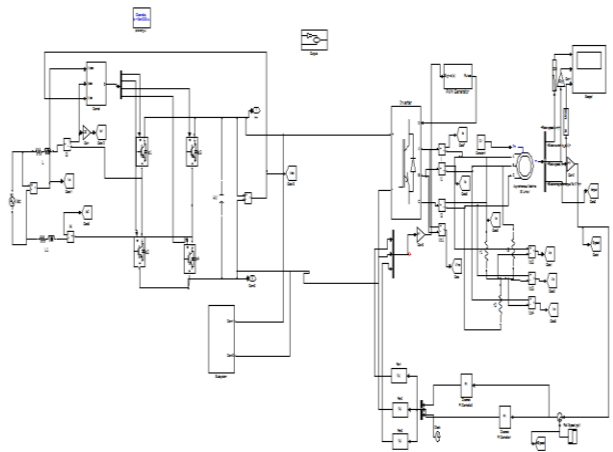
Rectifier Input Current i_{g2}



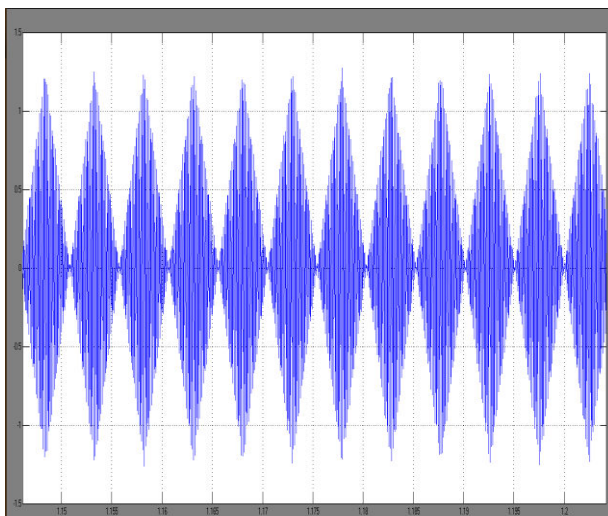
Load currents i_{s1} , i_{s2} and i_{s3}



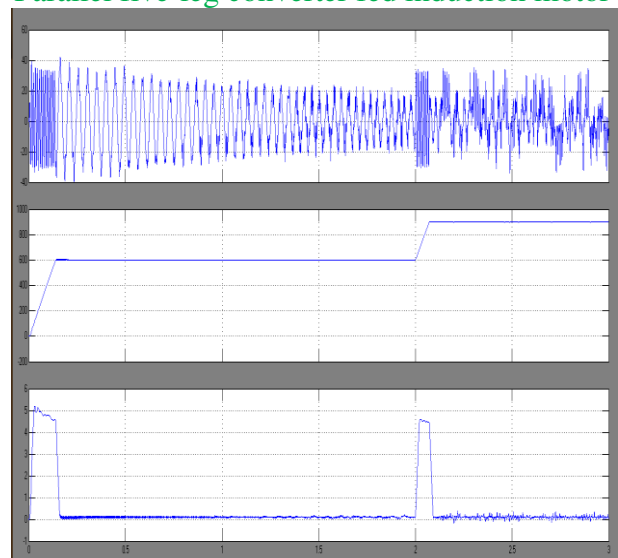
Dc-link total output voltage



MATLAB/SIMULINK circuit for 1ph-to-3ph converter using a half-bridge rectifier with Parallel five-leg converter fed induction motor



Circulating current



Induction motor current, Speed and Torque

IX. CONCLUSION

In this project, two drive motor systems have been presented. These systems are composed of an ac-dc-ac single-phase to three-phase converter. The single-phase rectifier combines two parallel single-phase half-bridge converters without transformers. Suitable model and control strategy, including the PWM strategy have been developed. The results for P5L and P4L configurations were obtained with double-carrier PWM, the condition that guarantees the lowest harmonic distortion. Among these configurations, the P5L topology presents the best performance, because it reduces: 1) power losses, due to a reduction of the rectifier currents and 2) the harmonic distortion on the utility grid, when the interleaved technique is applied. Furthermore, this configuration uses only 15% more of dc-link voltage rating than the conventional 5L converter. Three phase asynchronous induction motors are widely used in industrial applications due to their features of low cost, high reliability and less maintenance. The Photo Voltaic powered three phase induction motor drive system is successfully designed, modeled and simulated using Matlab/Simulink. The speed and efficiency of the system is improved.

REFERENCES

- [1] D.-C. Lee and Y.-S. Kim, "Control of single-phase-to three-phase AC/DC/AC PWM converters for induction,"
- [2] Cheng P-T, Hou C-C and Li J-S (2008), "Design of an Auxiliary Converter for the Diode Rectifier and the Analysis of the Circulating Current", IEEE Trans. Power Electron., Vol. 23, No. 4, pp. 1658-1667.
- [3] C. B. Jacobina, E. C. dos Santos Jr., E. R. C. da Silva, M. B. R. Correa, A. M. N. Lima, and T. M. Oliveira, "Reduced switch count multiple three phase ac machine drive systems," IEEE Trans. Power Electron., vol. 23, no. 2, pp. 966-976.
- [4] C. B. Jacobina, E. C. dos Santos Jr., E. R. C. da Silva, M. B. R. Correa, A. M. N. Lima, and T. M. Oliveira, "Reduced switch count multiple three-phase ac machine drive systems," IEEE Trans. Power Electron., vol. 23, no. 2, pp. 966-976, Mar. 2008.
- [5] D.-C. Lee and Y.-S. Kim, "Control of single-phase-to-three-phase AC/DC/AC PWM converters for induction motor drives," IEEE Trans. Ind. Electron., vol. 54, no. 2, pp. 797-804, Apr. 2007.
- [6] L. Woo-Cheol, L. Taek-Kie, and H. Dong-Seok, "A three phase parallel active power filter operating with PCC voltage compensation with consideration for an unbalanced load," IEEE Trans. Power Electron., vol. 17, no. 5, pp. 807-814, Sep. 2002.
- [6] P. Enjeti and A. Rahman, "A new single phase to three phase converter with active input current shaping for low cost AC motor drives," IEEE Trans. Ind. Appl., vol. 29, no. 2, pp. 806-813, Jul./Aug. 1993.
- [7] D.-C. Lee and Y.-S. Kim, "Control of single phase-to-three-phase AC/DC/AC PWM converters for induction motor drives," IEEE Trans. Ind. Electron., vol. 54, no. 2, pp. 797-804, Apr. 2007.
- [8] J. R. Rodríguez, J. W. Dixon, J. R. Espinoza, J. Pontt, and P. Lezana, "PWM regenerative rectifiers: State of the art," IEEE Trans. Ind. Electron., vol. 52, no. 1, pp. 5-22, Feb. 2005.
- [9] J.-K. Park, J.-M. Kwon, E.-H. Kim, and B.-H. Kwon, "High-performance transformer less online UPS," IEEE Trans. Ind. Electron., vol. 55, no. 8, pp. 2943-2953, Aug. 2008.
- [10] Z. Ye, D. Boroyevich, J.-Y. Choi, and F. C. Lee, "Control of circulating current in two parallel three-phase boost rectifiers," IEEE Trans. Power Electron., vol. 17, no. 5, pp. 609-615, Sep. 2002.



- [11] S. K. Mazumder, —Continuous and discrete variable-structure controls for parallel three-phase boost rectifier, IEEE Trans. Ind. Electron., vol. 52, no. 2, pp. 340–354, Apr. 2005.
- [12] R. Q. Machado, S. Buso, and J. A. Pomilio, “A line-interactive single-phase to three-phase converter system,” IEEE Trans. Power Electron., vol. 21, no. 6, pp. 1628–1636, May 2006.
- [13] O. Ojo, W. Zhiqiao, G. Dong, and S. Asuri, “High-performance speed-sensorless control of an induction motor drive using a minimalist single-phase PWM converter,” IEEE Trans. Ind. Appl., vol. 41, no. 4, pp. 996–1004, Jul. /Aug. 2005.